The effects of composition upon the high-pressure behaviour of amphiboles: compression of gedrite to 7 GPa and a comparison with anthophyllite and proto-amphibole

F. Nestola[1,2,*], D. Pasqual[1], M. D. Welch[3] and R. Oberti[4]

[1] Dipartimento di Geoscienze, Università di Padova, via Gradenigo 6, 35131 Padova, Italy
[2] CNR Istituto di Geoscienze e Georisorse, UOS Padova, via Gradenigo 6, 35131 Padova, Italy
[3] Department of Mineralogy, The Natural History Museum, Cromwell Road, London SW7 5BD, UK
[4] CNR Istituto di Geoscienze e Georisorse, UOS Pavia, via Ferrata 1, 27100 Pavia, Italy

ABSTRACT

A single-crystal X-ray diffraction study of a sample of natural gedrite from North Carolina, USA, with the crystal-chemical formula $^A Na_{0.47}{}^B(Na_{0.03}Mg_{0.97}Fe^{2+}_{0.94}Mn_{0.02}Ca_{0.04})^C(Mg_{3.52}Fe^{2+}_{0.28}Al_{1.15}Ti^{4+}_{0.05})$ $^T(Si_{6.31}Al_{1.69})O_{22}{}^W(OH)_2$, up to a maximum pressure of 7 GPa, revealed the following bulk and axial moduli and their pressure derivatives: $K_{0T} = 91.2(6)$ GPa [$K_{0T}' = 6.3(2)$]; $K_{0T}(a) = 60.5(6)$ GPa [$K_{0T}(a)' = 6.1(2)$]; $K_{0T}(b) = 122.8(2.6)$ GPa [$K_{0T}(b)' = 5.7(8)$]; $K_{0T}(c) = 119.7(1.5)$ GPa [$K_{0T}(c)' = 5.1(5)$]. Gedrite has a much higher bulk modulus than anthophyllite (66 GPa) and proto-amphibole (64 GPa). All of the three axial moduli of gedrite are higher than those of these two other ortho-amphiboles. The greater stiffness of gedrite along [100] is due to its high $^A Na$ content, which is almost zero in anthophyllite and proto-amphibole. The much greater stiffness parallel to the (100) plane of gedrite compared with the two other amphiboles is probably due to its high $^C Al$ content. A comparison is made with published data available for orthorhombic $^B(Mg,Mn,Fe)$ and monoclinic $^B Ca$ amphiboles to identify correlations between crystal-chemistry and compressibility in amphiboles.

Introduction

COMPRESSIBILITY and thermal expansivity are fundamental thermodynamic parameters that relate directly to the stability of a mineral assemblage. Despite their importance, few compressibilities and expansivities have been determined for amphiboles (Welch *et al.*, 2007). Although the primary goal of compression studies is to determine the bulk modulus (inverse compressibility, β^{-1}) of a phase, other valuable information is contained within the set of elastic constants. Diffraction studies which measure the variation of unit-cell parameters with pressure allow the derivation of bulk and axial moduli K_{0T}, $K_{0T}(a)$, $K_{0T}(b)$ and $K_{0T}(c)$, where the final brackets refer to values in different crystallographic directions. Superior datasets also allow the pressure derivatives (K_{0T}', K_{0T}'', $K_{0T}'(a)$, $K_{0T}''(a)$...) of these elastic moduli to be calculated. In highly topologically anisotropic phases such as amphiboles and sheet silicates, the principal crystallographic axes relate to key structural directions defined by silicate chains or sheets. In these cases the axial moduli can give insights into compression mechanisms, even if full structural refinements at high P cannot be obtained due to structural complexity and instrumental limitations in the angular range for data collection.

The effect of composition on thermodynamic properties is of particular interest in the earth sciences as it provides information which is valuable for modelling the Earth's interior. The thermodynamics of solid solutions is particularly relevant to petrological studies. For example, the question as to whether or not amphibole solid solutions are thermodynamically ideal at geological P and T is still open. Very few thermodynamic studies of binary or near-binary amphibole solid solutions have been reported: fluoro-[tremolite−edenite] was studied by Graham and Navrotsky (1986), and tremolite–richterite by Pawley *et al.* (1990). These measurements were made at ambient conditions, and their relevance to amphibole stability at high P and T is unclear. Volume is a thermodynamic quantity that can be used to quantify solid-solution behaviour (ideality *vs.* non-ideality via ΔV_{mix}). The determination of the bulk modulus, K_{0T}, from compression studies allows the volume at high P (and T, if expansivity data are available) to be calculated. If the bulk moduli across a solid solution can be measured, the pressure dependence of ΔV_{mix} can be determined. However, given the number of distinct samples that are required for this type of study (at least 7), the collection of such data is time consuming and is only possible on a realistic timescale using synchrotron X-ray powder diffraction on well characterized synthetic samples. It is, nonetheless, a worthwhile objective as little is known about the thermodynamics of amphiboles at mantle pressures. The first step is the acquisition of good compressibility and expansivity data for endmember amphiboles and other geologically relevant compositions.

In addition to providing quantitative data on amphibole solid solutions at high P and T, *in situ* high-P studies provide valuable insights into compression mechanisms. Using single crystals of good quality it is possible to quantify the pressure dependence of bulk and axial moduli, K' ($\partial K/\partial P$) and thereby predict structural hiatuses that may destabilize amphibole-group minerals at high P, or alternatively, stabilize them.

Solid solutions between the orthorhombic amphiboles gedrite, ideally $^A\square^B\mathrm{Mg}_2{}^C(\mathrm{Mg}_3\mathrm{Al}_2)^T(\mathrm{Si}_6\mathrm{Al}_2)\mathrm{O}_{22}{}^W(\mathrm{OH})_2$, and $^A\mathrm{Na}^B\mathrm{Mg}_2{}^C\mathrm{Mg}_5{}^T(\mathrm{Si}_7\mathrm{Al})\mathrm{O}_{22}{}^W(\mathrm{OH})_2$ (in the new classification scheme prepared by the subcommittee on amphiboles chaired by F.C. Hawthorne and R. Oberti and approved by IMA-CNMNC in April 2012), and their Fe(II)-substituted counterparts

(prefixed ferro-) are geologically relevant. Gedrites commonly contain significant $^A\mathrm{Na}$ (usually up to 0.5 atoms per formula unit, a.p.f.u.).

The crystal-chemistry of gedrite has been revised by Schindler *et al.* (2008) and Hawthorne *et al.* (2008). Zema *et al.* (2012) reported the high-T behaviour of a crystal from sample A(26) of Schindler *et al.* (2008), with a formula $^A\mathrm{Na}_{0.47}{}^B(\mathrm{Na}_{0.03}\mathrm{Mg}_{1.05}\mathrm{Fe}^{2+}_{0.86}\mathrm{Mn}_{0.02}\mathrm{Ca}_{0.04})^C(\mathrm{Mg}_{3.44}\mathrm{Fe}^{3+}_{0.36}\mathrm{Al}_{1.15}\mathrm{Ti}^{4+}_{0.05})^T(\mathrm{Si}_{6.31}\mathrm{Al}_{1.69})\mathrm{O}_{22}{}^W(\mathrm{OH})_2$, the structure of which is shown in Fig. 1. Orthorhombic *Pnma* amphiboles (e.g. anthophyllite and gedrite) contain two non-equivalent double-chains of tetrahedra, the A- and B-chains. Proto-amphibole, a much rarer orthorhombic structure, has space group *Pnmn* and two equivalent double-chains of tetrahedra. The Al contents of tetrahedra in the gedrite A(26) crystal studied by Zema *et al.* (2012) are as follows: $T1\mathrm{A} = 0.53$ a.p.f.u., $T2\mathrm{A} = 0.03$ a.p.f.u., $T1\mathrm{B} = 0.76$ a.p.f.u., $T2\mathrm{B} = 0.36$ a.p.f.u. The higher Al content of the B-chain results in larger tetrahedra and a more kinked chain. The ribbon of octahedrally coordinated edge-sharing $M1$, $M2$ and $M3$ sites is the least compressible component of the amphibole structure, and Zema *et al.* (2012) showed that in gedrite its thermal expansivity depends strongly on the oxidation state of Fe. In gedrite, $^C\mathrm{Al}$ is completely ordered at the smallest octahedrally coordinated site ($M2$) at the edge of the ribbon. At higher T, the $M4$ polyhedron loses almost all of its Fe, which migrates to the octahedrally coordinated sites and oxidizes to Fe^{3+}, leading to dehydrogenation (Zema *et al.*, 2012). The $M4$ polyhedron also deforms in response to rotation of the double-chains, which in turn respond to the deformation of the ribbon of octahedra. In general, larger $M4$ cations (e.g. Na and Ca in pargasite and richterite) resist compression more than smaller ones (Mg, Fe^{2+}). The A-cation is also expected to stiffen the structure across the channel perpendicular to (100), and indeed the thermal expansion coefficient α_a is smaller in gedrite A(26) $(1.11(1). \times 10^{-5}\ \mathrm{K}^{-1}$; Zema *et al.*, 2012) than in anthophyllite $(1.49 \times 10^{-5}\ \mathrm{K}^{-1}$; Welch *et al.*, 2011*a*).

Welch *et al.* (2011*b*) determined the bulk and axial moduli of a natural near-endmember anthophyllite with a formula $^A\mathrm{Na}_{0.04}{}^B(\mathrm{Mg}_{1.30}\mathrm{Mn}_{0.57}\mathrm{Ca}_{0.09}\mathrm{Na}_{0.04})^C(\mathrm{Mg}_{4.96}\mathrm{Fe}_{0.02}\mathrm{Al}_{0.02})^T(\mathrm{Si}_{7.99}\mathrm{Al}_{0.01})\mathrm{O}_{22}{}^W(\mathrm{OH})_2$ to 7 GPa, and compared these moduli with those of a natural proto-amphibole with a formula
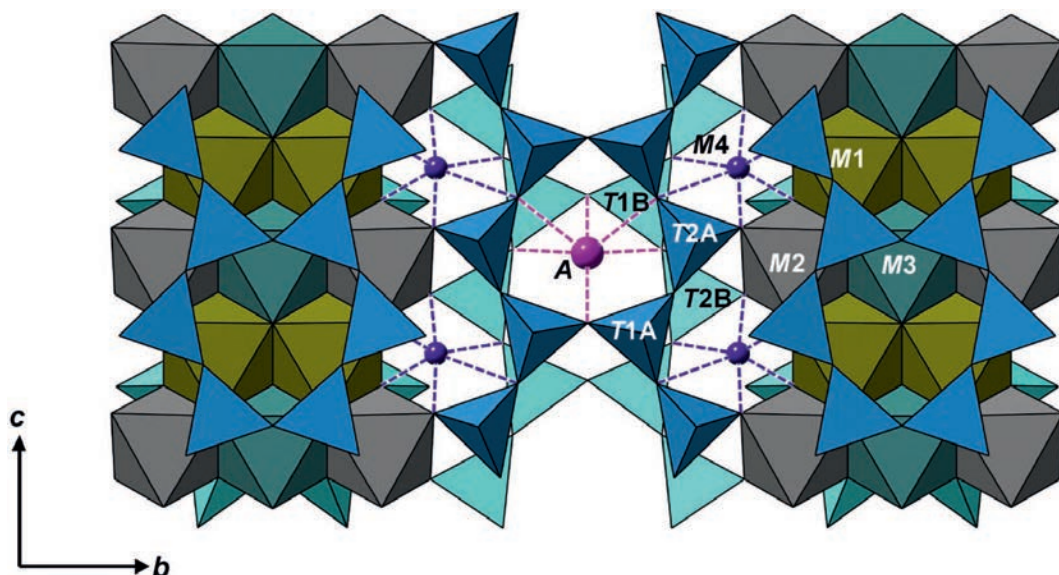
FIG. 1. The structure of gedrite (A26) projected onto (100), after Zema *et al*. (2012).

$^A\square\,^B(Mn_{1.39}Fe_{0.59})^C(Fe_{3.98}Mg_{1.02})^TSi_8O_{22}$ $^W(OH)_2$ reported by Zanazzi *et al*. (2010). It was concluded that the composition of the ribbon of edge-sharing octahedra, which is the most rigid component of the amphibole structure, exerts the main control upon compressibility. No significant symmetry effects (*Pnma vs*. *Pnmn*) on compressibility were identified.

As part of our ongoing research on the effects of composition on the physical behaviour of amphiboles, we have undertaken a high-*P* study of a gedrite crystal taken from the same sample as that used by Zema *et al*. (2012) for high-*T* studies. The crystal studied differs from the anthophyllite and proto-amphibole mentioned above in being Al-rich and having ^ANa ~0.5 a.p.f.u., thereby allowing the effects of the A-site, and *M* and *T*-site chemistry on compressibility to be evaluated.

Experimental Methods

The sample used in this study is from North Carolina, USA and has an original reference number AMNH 136484; it was listed as A(26) in the comprehensive review of gedrite crystal chemistry by Schindler *et al*. (2008). The single crystal selected for the high-pressure experiments $(0.05 \times 0.05 \times 0.15$ mm) was free of twins and inclusions, and showed sharp optical extinction and sharp Bragg reflections. It was from the same

group of gedrite crystals used by Schindler *et al*. (2008) and Zema *et al*. (2012) in their studies. Structure refinement of our gedrite A(26) prior to the high-*P* treatment showed substantial agreement with the sample studied by Zema *et al.* (2012), which has the crystal-chemical formula $^ANa_{0.47}\,^B(Na_{0.03}Mg_{1.05}Fe^{2+}_{0.86}Mn_{0.02}Ca_{0.04})$ $^C(Mg_{3.44}Fe^{2+}_{0.36}Al_{1.15}Ti^{4+}_{0.05})^T(Si_{6.31}Al_{1.69})O_{22}$ $^W(OH)_2$. The sample used in this study has a total of 107.85 electrons per formula unit (e.p.f.u.) for the *M*1−4 and A sites, compared to 107.30 e.p.f.u. for the crystal of Zema *et al*. (2012). There is a slightly different partitioning of Fe/Mg between the *M*4 and the *M*1−3 sites; when comparing refined site-scattering values and mean bond lengths, we estimate +0.08 $^BFe^{2+}$ and −0.08 $^CFe^{2+}$ a.p.f.u. for the crystal used in this work. The small crystal size and large number of structural parameters to be determined (110 for isotropic refinement), precluded reliable structure refinement of our high-pressure data.

After the ambient data collection, the crystal was loaded in an ETH-type diamond-anvil cell (Miletich *et al.*, 2000) using T301 steel foil as gaskets, which was pre-indented to 0.090 mm and a 0.25 mm diameter cylindrical hole was drilled into it by spark-erosion. A crystal of quartz was used as an internal pressure standard (Angel *et al*., 1997). A 4:1 methanol:ethanol mixture was used as the pressure medium, as it remains hydrostatic

up to the maximum pressure reached in the experiment (Angel *et al.*, 2007). The high-*P* experiments were performed on a STOE STADI IV single-crystal diffractometer with a full χ-circle operating at 50 kV and 40 mA, using Mo*K*α radiation and a point detector. Data collection was controlled by the *SINGLE* program (Angel and Finger, 2011) with eight-position centring to produce accurate and precise data (Angel *et al.*, 2000; Nestola *et al.*, 2005, 2006). A few overlapping of reflections from amphibole and diamond were identified and masked. Unit-cell parameters were obtained by least-squares refinement in orthorhombic (*Pnma*) symmetry. Bulk and axial moduli and their first pressure derivatives were derived from the unit-cell parameters using *EOSFIT5.2* software (Angel, 2000).

Results

The unit-cell parameters were obtained from eight-position centring of at least 35 reflections up to $\theta_{max} = 35º$ at each pressure value (Table 1). Eulerian strain (*f*) was plotted against normalized pressure (*F*) (Birch, 1978; Angel, 2000) to establish whether or not fitting to a third-order Birch-Murnaghan equation of state (BM3 EoS) was justified (Birch, 1947). The clear deviation from a horizontal line (Fig. 2) indicates that a pressure dependence should be refined to obtain the first derivatives of bulk and axial moduli. Consequently, we fitted the data to a BM3 EoS of the general form:

$$P = \frac{3K_T}{2} \left[\left(\frac{V_0}{V_P}\right)^{\frac{7}{3}} - \left(\frac{V_0}{V_P}\right)^{\frac{5}{3}} \right]$$
$$\left(1 + \frac{3(K_T' - 4)}{4} \left(\left(\frac{V_0}{V_P}\right)^{\frac{2}{3}} - 1 \right) \right)$$

Fits of the variation of the unit-cell parameters with *P* using a BM3 EoS are shown in Fig. 3, and the absolute volume data are shown in Fig. 4. Elastic moduli of gedrite A(26) are given in Table 2 and compression curves for *a*, *b*, *c* and *V* calculated from these elastic moduli are plotted in Fig. 5. We evaluate these elastic moduli with reference to related amphiboles in the following section.

Discussion

The elastic moduli of gedrite A(26), $^A\text{Na}_{0.47}$ $^B(\text{Na}_{0.03}\text{Mg}_{1.05}\text{Fe}^{2+}_{0.94}\text{Mn}_{0.02}\text{Ca}_{0.04})$ $^C(\text{Mg}_{3.44}\text{Fe}^{2+}_{0.28}\text{Al}_{1.15}\text{Ti}^{4+}_{0.05})^T(\text{Si}_{6.31}\text{Al}_{1.69})\text{O}_{22}$ $^W(\text{OH})_2$, from this study, anthophyllite, $^A\text{Na}_{0.01}$ $^B(\text{Mg}_{1.30}\text{Mn}_{0.57}\text{Ca}_{0.09}\text{Na}_{0.04})^C(\text{Mg}_{4.95}\text{Fe}_{0.02}$ $\text{Al}_{0.03})^T\text{Si}_8\text{O}_{22}{}^W(\text{OH})_2$, from Welch *et al.* (2011*b*) and the proto-amphibole proto-ferro-mangano-anthophyllite (PMFA), $^A\square^B(\text{Mn}_{1.39}\text{Fe}_{0.59})$ $^C(\text{Fe}_{3.98}\text{Mg}_{1.02})^T\text{Si}_8\text{O}_{22}{}^W(\text{OH})_2$, from Zanazzi *et al.* (2010) are listed in Table 2 and are compared in Fig. 5. Anthophyllite and PMFA, despite their differing ratios of large and small octahedrally coordinated cations [(Fe,Mn)/Mg] and their different crystal symmetry, have similar bulk and axial moduli. However, the first pressure

TABLE 1. Unit-cell parameters and volume at different pressures measured for gedrite A(26). The errors are in parentheses.

| *P* (GPa)	*a* (Å)	*b* (Å)	*c* (Å)	*V* (Å^3)
0.00010(1)	18.5418(8)	17.8067(8)	5.2714(2)	1740.45(13)
0.838(7)	18.4594(9)	17.7668(9)	5.2589(3)	1724.75(15)
0.976(8)*	18.4473(7)	17.7597(7)	5.2569(4)	1722.26(14)
1.703(7)	18.3825(7)	17.7280(7)	5.2469(3)	1709.88(13)
2.359(7)	18.3269(8)	17.7013(8)	5.2383(3)	1699.35(15)
3.135(8)*	18.2649(7)	17.6649(7)	5.2280(3)	1686.81(14)
3.722(9)	18.2205(8)	17.6428(8)	5.2212(2)	1678.40(13)
4.720(9)*	18.1523(9)	17.5990(9)	5.2080(6)	1663.77(21)
5.530(10)*	18.0941(7)	17.5699(6)	5.1989(3)	1652.80(13)
6.230(12)*	18.0486(7)	17.5429(7)	5.1912(4)	1643.64(16)
7.045(21)	18.0047(8)	17.5174(9)	5.1804(4)	1633.86(18)

* Data measured during decompression.
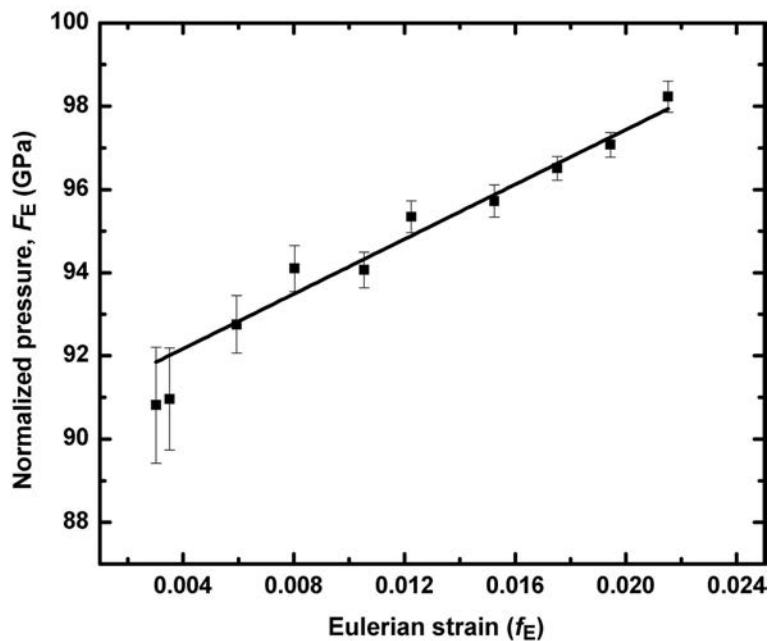
FIG. 2. Plot of normalized pressure (F_E) *vs.* Eulerian strain (f_E) for gedrite A(26). The clear non-zero slope of these data indicates that fitting to a third-order Birch−Murnaghan EoS is required.
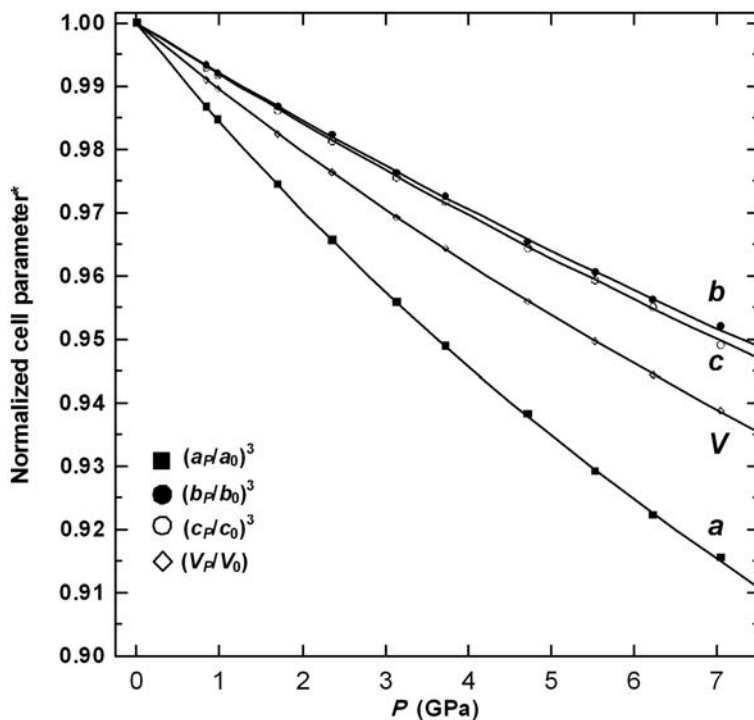

FIG. 3. The variations of the gedrite unit-cell parameters expressed as x_P/x_0, where x_0 is the value of the parameter at 0.0001 GPa, with pressure, fitted to a third-order Birch−Murnaghan EoS.
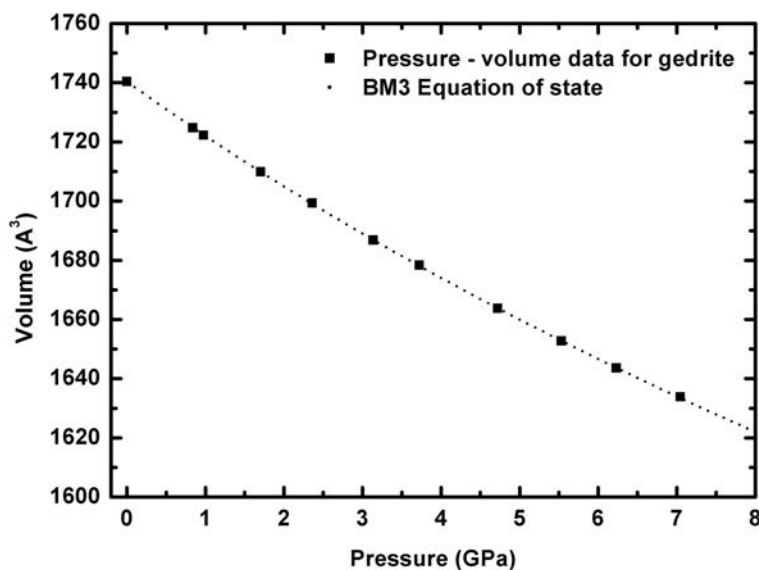
FIG. 4. The variation of the unit-cell volume of gedrite A(26) with pressure fitted with the same third-order Birch−Murnaghan EoS used in Fig. 3.

derivatives parallel to the (100) plane, $K_{0T}(b)'$ and $K_{0T}(c)'$, are very different for the two amphiboles, with anthophyllite stiffening with P at a much great rate than PMFA. Welch *et al.* (2011*b*)

proposed that this difference was due to the very different Mg/Fe^{2+} ratios in the two amphiboles, as the smaller Mg octahedra resist compression more than the Fe^{2+} octahedra.

TABLE 2. A compilation of bulk and axial moduli for orthorhombic amphiboles.

	Gedrite A(26)	Anthophyllite	PMFA	Kaersutite	Pargasite	Tremolite
V_0 (Å^3)	1740.39(12)	1766.07(3)	926.4(4)	903.6(2)	906.6	905.8
K_{0T} (GPa)	91.2(6)	66(2)	64(1)	94(1)	91(6)	76(3)
K'	6.3(2)	11(1)	7.0(4)	6.3(4)		
a_0 (Å)	18.5419(11)	18.583(7)	9.430(2)	9.815(2)	9.533(1)*	9.515(1)*
K_{0T} (GPa)	60.5(6)	41(3)	30.7(8)	86(3)	58(3)*	47(2)*
K'	6.1(2)	11(2)	10.8(5)	7(1)		
b_0 (Å)	17.8069(12)	17.990(3)	18.364(4)	18.012(2)	17.998(1)	18.042(1)
K_{0T} (GPa)	122.8(2.6)	97(5)	109(4)	115(3)	122(4)	106(10)
K'	5.7(8)	6(2)	2.7(8)	4.8(8)		
c_0 (Å)	5.2712(2)	5.283(2)	5.354(2)	5.300(1)	5.284(1)	5.276(1)
K_{0T} (GPa)	119.7(1.5)	83(7)	94(5)	112(5)	134(10)	122(23)
K'	5.1(5)	12(4)	4(1)	7(1)		

Data sources are as follows: gedrite A(26) (this study); anthophyllite (Welch *et al.*, 2011*b*); proto-mangano-ferro-anthophyllite, PMFA (Zanazzi *et al.*, 2010); kaersutite (FR12) (Comodi *et al.*, 2010); pargasite and tremolite (Comodi *et al.*, 1991 recalculated by Welch *et al.*, 2007). Unit-cell volume and *a*, *b* and *c* cell parameters for the first four samples were fitted to a third-order Birch−Murnaghan equation of state, those of tremolite and pargasite were fitted to a second-order Birch−Murnaghan equation of state.
* The "*a* parameter" values used for the monoclinic amphiboles correspond to the behaviour of *a*sinβ.
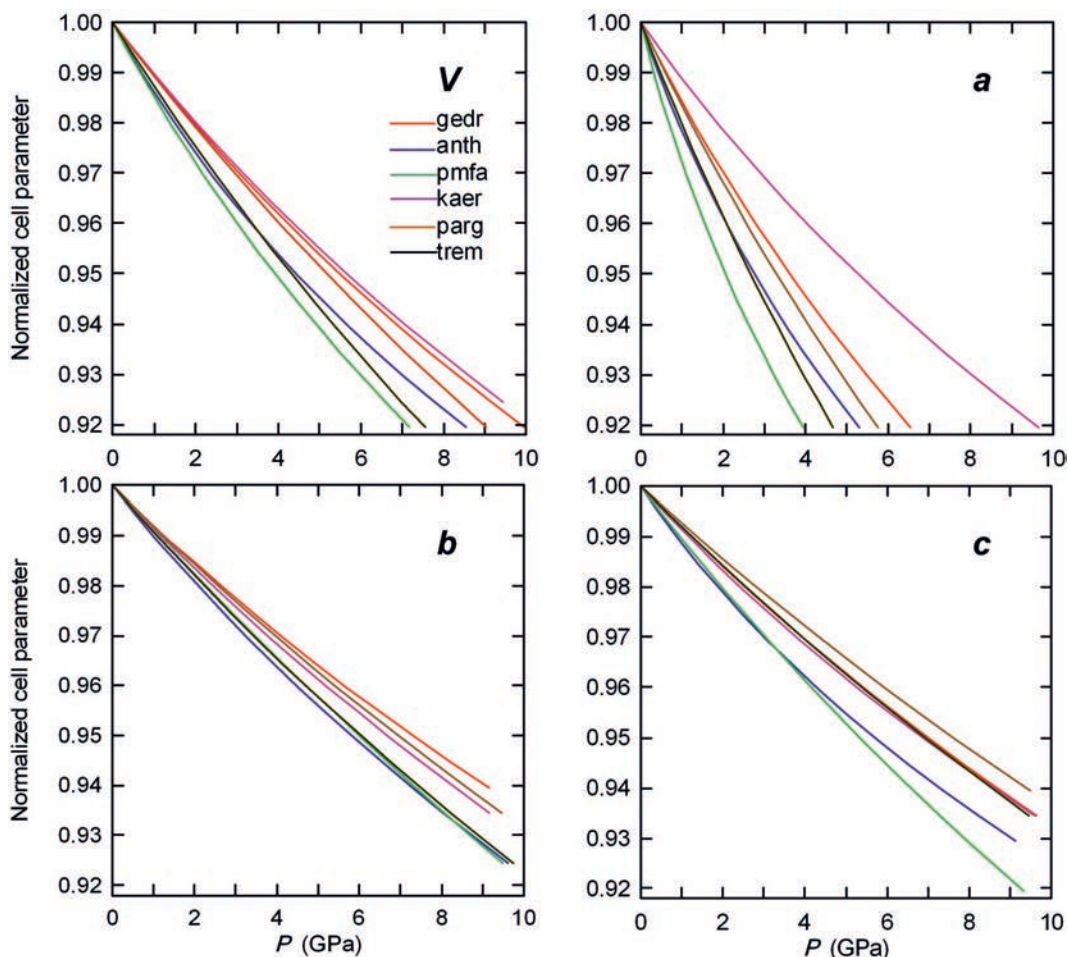
FIG. 5. Comparative compressibility data for amphiboles. Abbreviations are as follows: gedr = gedrite A(26), ^{A}Na$_{0.47}$ ^{B}(Na$_{0.03}$Mg$_{1.05}$Fe$^{2+}_{0.94}$Mn$_{0.02}$Ca$_{0.04}$)^C(Mg$_{3.44}$Fe$^{2+}_{0.28}$Al$_{1.15}$Ti$^{4+}_{0.05}$)^T(Si$_{6.31}$Al$_{1.69}$)O$_{22}$^{W}(OH)$_2$ (this study); anth = antho-phyllite, ^{A}Na$_{0.01}$^{B}(Mg$_{1.30}$Mn$_{0.57}$Ca$_{0.09}$Na$_{0.04}$)^C(Mg$_{4.95}$Fe$_{0.02}$Al$_{0.03}$)^{T}Si$_8$O$_{22}$^{W}(OH)$_2$ (Welch *et al*., 2011a); pmfa = proto-ferro-mangano-anthophyllite, ^{A}□^{B}(Mn$_{1.39}$Fe$_{0.59}$)^C(Fe$_{3.98}$Mg$_{1.02}$)^{T}Si$_8$O$_{22}$^{W}(OH)$_2$ (Zanazzi *et al*., 2010); kaer = kaersutite FR12, ^{A}(K$_{0.29}$Na$_{0.68}$Ca$_{0.03}$)^B(Ca$_{1.79}$Mg$_{0.21}$)^C(Mg$_{2.65}$Fe$^{2+}_{0.05}$Mn$^{2+}_{0.01}$Fe$^{3+}_{1.27}$Ti$_{0.59}$Al$_{0.43}$)^T(Si$_{5.97}$Al$_{2.03}$)O$_{22}$ ^{W}(OH$_{0.07}$F$_{0.04}$O$_{1.89}$) (Comodi *et al*., 2010); parg = pargasite DL5, ^{A}(K$_{0.02}$Na$_{0.74}$)^B(Ca$_{1.98}$Fe$^{2+}_{0.02}$)^C(Mg$_{4.26}$Fe$^{2+}_{0.19}$Cr$_{0.18}$ Ti$_{0.07}$Al$_{0.30}$)^T(Si$_{6.62}$Al$_{1.38}$)O$_{22}$^{W}(OH)$_2$; and trem = tremolite ^{A}□^{B}Ca$_2$^{C}(Mg$_{4.95}$Fe$^{2+}_{0.05}$)^{T}Si$_8$O$_{22}$^{W}(OH)$_2$ (Comodi *et al.*, 1991, recalculated by Welch *et al.* 2007). Based upon the data reported in the respective studies, curves shown for tremolite and pargasite are calculated using second-order Birch−Murnaghan equations of state, whereas those of the three orthorhombic amphiboles and kaersutite are calculated using third-order Birch−Murnaghan equations of state.

Note that the "*a* parameter" values used for the monoclinic amphiboles correspond to the behaviour of *a*sinβ.

The gedrite crystal studied in this work has a much higher bulk modulus (92 GPa) than anthophyllite (66 GPa) and PMFA (64 GPa). All three axial moduli of gedrite A(26) are higher than those of the other two amphiboles. The greater stiffness of gedrite A(26) along [100] is due to its high ^{A}Na content (0.47 a.p.f.u.), which is almost zero in anthophyllite and PMFA. The greater stiffness of gedrite A(26) parallel to the (100) plane compared with the other two orthorhombic amphiboles is probably due to the high ^{C}Al content (1.15 a.p.f.u.). Consequently, $M2$ is the least compressible octahedron and imparts considerable overall rigidity to the ribbon.

In contrast, in anthophyllite $M2$ (Mg) is the most compressible octahedron (Welch et al., 2011b). We also note that Zema et al. (2012) found that the $M2$ octahedron of gedrite A(26) is half as expandable as the $M1$ and $M3$ octahedra.

The $^CFe^{2+}$ content of gedrite A(26) (0.36 a.p.f.u.) is higher than that of anthophyllite (0.02 a.p.f.u.; Welch et al., 2011a), but much lower than that of PMFA (3.98 a.p.f.u.; Zanazzi et al., 2010). Therefore, the greater stiffness of gedrite parallel to the (100) plane reflects its high ^CAl, which more than compensates for the lower $^CFe^{2+}$ content.

Some further inferences on the compositional effects on compressibility in amphiboles can be drawn by comparing gedriteA(26)/anthophyllite with pargasite/tremolite (Table 2; Fig. 5). The primary compositional difference between these orthorhombic and monoclinic amphiboles concerns the B cations, which are dominated by small cations (Mg, Fe^{2+}, Mn^{2+}) in gedrite A(26)/ anthophyllite, but by a large cation, Ca, in pargasite/tremolite. The compositional differences between anthophyllite (Welch et al. 2011a) and gedrite A(26) are the same as those between endmember tremolite and pargasite, i.e. changes in ^ANa, ^CAl and ^TAl contents. A comparison can therefore be made with the compressibility data of Comodi et al. (1991) for tremolite, $^A\square^BCa_2{}^C(Mg_{4.95}Fe^{2+}_{0.05})^TSi_8O_{22}$ $^W(OH)_2$, and pargasite, $^A(K_{0.02}Na_{0.74})$ $^B(Ca_{1.98}Fe^{2+}_{0.02})^C(Mg_{4.26}Fe^{2+}_{0.19}Cr_{0.18}Ti_{0.07}Al_{0.30})$ $^T(Si_{6.62}Al_{1.38})O_{22}{}^W(OH)_2$, measured up to 4 GPa, and also with the kaersutite (FR12) of Comodi et al. (2010), $^A(K_{0.29}Na_{0.68}Ca_{0.03})^B(Ca_{1.79}Mg_{0.21})$ $^C(Mg_{2.65}Fe^{2+}_{0.05}Mn^{2+}_{0.01}Fe^{3+}_{1.27}Ti_{0.59}Al_{0.43})^T(Si_{5.97}$ $Al_{2.03})O_{22}{}^W(OH_{0.07}F_{0.04}O_{1.89})$, measured up to 7 GPa.

In terms of their elastic behaviour two distinct groups of amphiboles are evident in Fig. 5: a gedrite-kaersutite-pargasite group and an anthophyllite-PMFA-tremolite group. That the behaviour of gedrite is similar to that of kaersutite and pargasite is consistent with its high A-site occupancy and ^CAl content, which contrasts with the vacant A sites and the very low Al contents of tremolite, anthophyllite and PMFA. The stiffening effect of A-site occupancy by Na and K is most clearly seen in the behaviour of the a parameter ($a\sin\beta$ in monoclinic amphiboles). The a-parameter curves of the anthophyllite-PMFA-tremolite group lie well below those of the gedrite-kaersutite-pargasite group. The clearest distinction between the two groups is

shown by the behaviour of the b parameter, reflecting the importance of the nature of the C cations (in particular Al) in stiffening the amphibole structure. Tremolite is similar to the gedrite-kaersutite-pargasite group in the behaviour of its c parameter on compression, perhaps reflecting its high ^BCa content (a large cation) which resists compression and may compensate for the absence of ^CAl. Overall, it is clear that the elastic properties of gedrite are more like those of kaersutite and pargasite than those of the other orthorhombic amphiboles or tremolite, showing the importance of the A-site and ^CAl in stiffening the amphibole structure.

Acknowledgements

References

Angel, R.J. (2000) Equations of State. Pp. 35–39 in: High-temperature and high-pressure crystal chemistry (R.M. Hazen and R.T. Downs, editors). Reviews in Mineralogy and Geochemistry, **41**. Mineralogical Society of America, Washington DC and the Geochemical Society, St Louis, Missouri, USA.

Angel, R.J. and Finger, L.W. (2011) SINGLE: a program to control single-crystal diffractometers. Journal of Applied Crystallography, **44**, 247–251.

Angel, R.J., Allan, D.R., Miletich, R. and Finger, L.W. (1997) The use of quartz as an internal pressure standard in high-pressure crystallography. Journal of Applied Crystallography, **39**, 461–466.

Angel, R.J., Downs, R.T. and Finger, L.W. (2000) High-temperature–high-pressure diffractometry. Pp.

247−251 in: *High-temperature and High-pressure Crystal Chemistry* (R.M. Hazen and R.T. Downs, editors). Reviews in Mineralogy and Geochemistry, **41**. Reviews in Mineralogy and Geochemistry, **41**. Mineralogical Society of America, Washington DC and the Geochemical Society, St Louis, Missouri, USA.

Angel, R.J., Bujak, M., Zhao, J., Gatta, G.D. and Jacobsen, S.D. (2007) Effective hydrostatic limits of pressure media for high-pressure crystallographic studies. *Journal of Applied Crystallography*, **40**, 26−32.

Birch, F. (1947) Finite elastic strain of cubic crystals. *Physical Review*, **71**, 809−824.

Birch, F. (1978) Finite strain isotherm and velocities for single-crystal and polycrystalline NaCl at high pressure and 300 K. *Journal of Geophysical Research*, **83**, 1257−1268.

Comodi, P., Mellini, M., Ungaretti, L. and Zanazzi, P.F. (1991) Compressibility and high-pressure structure refinement of tremolite, pargasite and glaucophane. *European Journal of Mineralogy*, **3**, 485−499.

Comodi, P, Boffa Ballaran, T., Zanazzi, P.F., Capalbo, C., Zanetti, A. and Nazzareni, S. (2010) The effect of oxo-component on the high-pressure behavior of amphiboles. *American Mineralogist*, **95**, 1042−1051.

Graham, C.M. and Navrotsky, A. (1986) Thermochemistry of the tremolite-edenite amphiboles using fluorine analogs, and applications to amphibole-plagioclase-quartz. *Contributions to Mineralogy and Petrology*, **93**, 18−32.

Hawthorne, F.C., Schindler, M., Abdu, Y., Sokolova, E., Evans, B.E. and Ishida, K. (2008) The crystal-chemistry of gedrite-group amphiboles. II. Stereochemistry and chemical relations. *Mineralogical Magazine*, **72**, 731−745.

Miletich, R., Allan, D.R. and Kuhs, W.F. (2000) High-pressure single-crystal techniques. Pp. 445−519 in: *High-temperature and High-pressure Crystal Chemistry* (R.M. Hazen and R.T. Downs, editors). Reviews in Mineralogy and Geochemistry, **41**. Mineralogical Society of America, Washington DC and the Geochemical Society, St Louis, Missouri, USA.

Nestola, F., Boffa Ballaran, T., Tribaudino, M. and Ohashi, H. (2005) Compressional behaviour of $CaNiSi_2O_6$ clinopyroxene: bulk modulus systematics and cation type in clinopyroxenes. *Physics and Chemistry of Minerals*, **32**, 222−227.

Nestola, F., Boffa Ballaran, T., Liebske, C., Bruno, M. and Tribaudino, M. (2006) High-pressure behaviour along the jadeite $NaAlSi_2O_6$−aegirine $NaFeSi_2O_6$ solid solution up to 10 GPa. *Physics and Chemistry of Minerals*, **33**, 417−425.

Pawley, A.R., Graham, C.M. and Navrotsky, A. (1990) Tremolite-richterite amphiboles: synthesis, compositional and structural characterization, and thermochemistry. *American Mineralogist*, **78**, 23−35.

Schindler, M., Sokolova, E., Abdu, Y., Hawthorne, F.C., Evans, B.E. and Ishida, K. (2008) The crystal-chemistry of the gedrite-group amphiboles. I. Crystal structure and site populations. *Mineralogical Magazine*, **72**, 703−730.

Welch, M.D., Cámara, F., Della Ventura, G. and Iezzi, G. (2007) Non-ambient *in situ* studies of amphiboles. Pp. 223−260 in: *Amphiboles: Crystal Chemistry, Occurrence, and Health Issues* (F.C. Hawthorne, R. Oberti and G. Della Ventura, editors). Reviews in Mineralogy and Geochemistry, **67**. Mineralogical Society of America, Washington DC and the Geochemical Society, St Louis, Missouri, USA.

Welch, M.D., Cámara, F. and Oberti, R. (2011*a*) Thermoelasticity and high-*T* behaviour of anthophyllite. *Physics and Chemistry of Minerals*, **38**, 321−334.

Welch, M.D., Gatta, G.D. and Rotiroti, N. (2011*b*) The high-pressure behavior of orthorhombic amphiboles. *American Mineralogist*, **96**, 623−630.

Zanazzi, P.F., Nestola, F., and Pasqual, D. (2010) Compressibility of protoamphibole: a high-pressure single-crystal diffraction study of protomangano-ferro-anthophyllite. *American Mineralogist*, **95**, 1758−1764.

Zema, M., Welch, M.D. and Oberti, R. (2012) High-*T* behaviour of orthorhombic amphiboles: thermoelasticity, cation site-exchange and dehydrogenation in gedrite. *Contributions to Mineralogy and Petrology*, **163**, 923−937.